***Study design***. Cross-sectional study.

***Objective.*** To assess the inter- and intraobserver reliability of thoracic, spino-pelvic and rod lengthening measurements in children treated with magnetically controlled growing rod (MCGR) using biplanar spinal stereoradiography (EOS imaging).

***Summary of background data.*** EOS imaging is widely used for diagnosis and monitoring of children with Early Onset Scoliosis. However, there is a paucity of literature on the reliability of thoracic and spino-pelvic parameters on EOS imaging in children treated with MCGR.

***Methods***. Three independent reviewers independently read a random assortment of 20 whole spine posteroanterior and lateral radiographs from patients treated with MCGR. The measurements were repeated four weeks after the initial read. The following radiological parameters were measured: Cobb angle of the main and compensatory curves, coronal balance, coronal T1-S1 and T1-T12 length, chest width and depth at T6, pelvic inlet width, MCGR distracted lengths, global kyphosis, proximal and distal junctional angle, lordosis, sagittal balance, pelvic incidence, pelvic tilt and sacral slope. Statistical analysis was performed with paired t-test and Cronbach's alpha for inter- and intraobserver reliability.

***Results***. All measurements had good or excellent intra- and interobserver reliability ($\alpha>0.8$; $p<0.05$), except measurements of the proximal junctional angle which showed only poor intra- and interobserver reliability for patients with an UIV cranial to T4.

**Conclusion**. EOS imaging is reliable for diagnosis and monitoring of children with Early Onset Scoliosis treated with MCGR. EOS imaging is particularly excellent for assessment of MCGR lengthening. Diagnosis and interpretation of early PJK within the cervicothoracic junction should be made with caution.

## INTRODUCTION

Scoliosis that presents before the age of ten is defined as Early Onset Scoliosis. The etiology of Early Onset Scoliosis can be classified as idiopathic, congenital, neuromuscular or syndromic. Treatment of these deformities is challenging as early spinal fusion leads to significant inhibition of spine and thoracic growth resulting in pulmonary underdevelopment, loss of the normal proportionality of trunk growth, and the potential development of crankshaft phenomenon [1]. Therefore, current treatment strategies aim for growth-sparing techniques to accommodate for thoracic and spinal growth and prevent the sequelae of early fusion surgery. Traditional growing rods allow periodic distraction to preserve spinal growth but necessitate regular surgery for open distractions which is associated with significant wound and anesthestic complications [2, 3]. Magnetically controlled growing rods (MCGR) have been developed to avoid such complications by non-invasive outpatient based distractions. MCGRs are well established regarding their safety and effectiveness, and there have been advances in ultrasound assessment of distractions and an extended role with gradual correction of severe deformities [4–15]. Despite advances with using ultrasound for monitoring distractions, radiographs at regular intervals are still required to verify rod lengthening and to detect complications such as proximal junctional kyphosis (PJK) or implant failure.

Monitoring of spino-pelvic and thoracic parameters is particularly important for accurate assessment of curve progression, spine and thoracic growth, and treatment outcomes with MCGR surgery. Slot scanning (EOS; EOS® imaging, Paris, France) imaging is associated with a significantly reduced radiation dose compared to conventional whole spine radiography [16, 17]. Therefore EOS imaging is gaining popularity for its ability to provide biplanar assessments of the whole body and spine at lower radiation exposure. However, there is a paucity of literature on the accuracy and reliability of EOS imaging in assessment

of spino-pelvic and thoracic measurements, and rod distraction lengths in children treated with MCGR. Hence, the aim of this study is to determine the reliability of various spino-pelvic and thoracic measurements with EOS imaging in patients undergoing treatment with MCGR.

## MATERIALS AND METHODS

A random assortment of 20 EOS whole spine biplanar radiographs from patients currently undergoing MCGR treatment was utilized for this study. Two patients were represented with two radiographs and one patient with three radiographs at different times. The study population included subjects with idiopathic (n=10), congenital (n=4), neuromuscular (n=1), and syndromic (n=2) scoliosis. At our institution, EOS radiographs are routinely acquired with patients standing relaxed, arms forward, and elbows flexed with the knuckles on clavicle position [18]. Three independent reviewers (two board certified orthopaedic surgeons and one research assistant) performed the measurements independently using Centricity Universal Viewer (GE Healthcare, Chicago, Illionois, USA) and were blinded to patient details. The following parameters were measured:

1. Cobb angle of the main and compensatory curves
2. Coronal balance was defined as the distance (mm) between the C7 plumb line and the Central Sacral Vertical Line (CSVL)
3. T1-12 and T1-S1 length were defined as the distance (mm) from the center of the upper endplate of the T1 vertebra to the center of the upper endplate of the T12 and S1 vertebrae, respectively (Figure 1)
4. Pelvic inlet width (mm) (Figure 2)
5. MCGR distracted length (mm) measured from the housing unit of the MCGR actuator (Figure 3)

6. Global thoracic kyphosis of T5 and T12
7. Lumbar lordosis of L1 and S1
8. Proximal Junctional Angle (PJA) defined as angle of the cranial segment adjacent to the instrumentation measured from the upper endplate of the vertebra cranial to the Upper Intrumented Vertebra (UIV) and the lower endplate of the UIV in the sagittal plane
9. Distal Junctional Angle (DJA) defined as angle of the caudal segment adjacent to the instrumentation measured from the lower endplate of the vertebra caudal to the Lower Intrumented Vertebra (LIV) and the upper endplate of the LIV in the sagittal plane
10. Sagittal Vertical Axis (SVA)
11. Chest depth and width at T6 were defined as the distance (mm) between the outer margins of the lung in anteroposterior and lateral projection, respectively, through the midpoint of the T6 vertebra (Figure 4)
12. Pelvic incidence (PI)
13. Pelvic tilt (PT)
14. Sacral slope (SS)

*Statistical analysis*

For intraobserver reliability the measurements were repeated four weeks after the initial reading. Paired t-test and Cronbach's alpha (α) were used for statistical analysis of inter- and intraobserver reliability. Reliability was defined as excellent ($0.9 \leq \alpha$), good ($0.8 \leq \alpha < 0.9$), acceptable ($0.7 \leq \alpha < 0.8$), questionable ($0.6 \leq \alpha < 0.7$), poor ($0.5 \leq \alpha < 0.6$), and unacceptable ($\alpha < 0.5$) [19].

**RESULTS**

Tables 1 and 2 provide an overview of inter- and intraobserver reliability. All parameters under study showed good or excellent inter- and intraobserver reliability ($\alpha>0.8$; $p<0.05$), except PJA, which showed poor interobserver reliability ($\alpha<0.6$; $p<0.05$) and unacceptable intrabserver reliability ($\alpha<0.5$; $p<0.54$).

A subgroup analysis including only patients where the UIV is caudal to T4 shows that within this group the reliability for PJA increases. In this subgroup the interobserver reliability is good ($\alpha>0.8$; $p<0.05$), but the intraobserver reliability is still poor ($\alpha<0.6$; $p<0.05$).

## DISCUSSION

This is the first study to evaluate inter- and intraobserver reliability of spino-pelvic and thoracic measurements in patients who underwent MCGR treatment using EOS imaging. This is an important study to determine whether we are performing reliable measurements for regular monitoring of treatment outcomes and complications in these early onset scoliosis patients. We found that EOS imaging in general provides a good platform as most measurements scored good or excellent reliability. This is especially important for patients treated with MCGR as distraction monitoring is crucial and our rod lengthening measurements were near perfect. As MCGR is usually indicated for early onset scoliosis, achieving excellent reliability for spino-pelvic and spine height parameters was also promising. Similar excellent reliability has been shown by Michael et al. for spine and thoracic height measurements in children with Early Onset Scoliosis [20].

PJA was found as the only measurement under investigation with poor reliability. In fact, intraobserver reliability for PJA was negative. This can be interpreted in two different ways. One situation in which negative reliability may occur is when the scale items represent more than one dimension of meaning. In this case a lordotic PJA will be defined as negative.

However, this scenario is less likely as no lordotic PJA was measured. A second possibility is when true reliability approaches zero with a relatively small study sample size. This may lead to a negative reliability coefficient because of a random disturbance in the data. The random disturbance or rather distribution of the measurements nicely reflects their poor reliability.

This finding has significant clinical impact as PJK is a common complication of growing rod treatment and accurate assessment of the PJA is necessary for diagnosis [21, 22]. Kwan et al. reported PJK with proximal junctional failure as one of the most common indications for revision surgery in MCGR treatment [23]. Our findings may suggest that complication rates of PJK may be poorly reported due to the difficulties in visualizing the PJA. Sagittal parameters involving high thoracic levels or the cervicothoracic junction like PJA may be difficult to identify properly in the sagittal plane due to poor visibility with overlap of the shoulders [24]. Accordingly, we found that for patients with an UIV caudal to T4 the reliability for PJA increases significantly. For these patients diagnosis of PJK may be easier and more accurate than for patients with a higher UIV cranial to T4. Visualization is further impaired if the instrumented levels are located within the deformity (Figure 5). The poor reliability of PJA may limit the ability of investigators to detect complications like PJK. As such, interval assessment of implant position may be more helpful to assess proximal junctional problems and coned view xray or computed tomography may be indicated in suspicious cases.

As this study was of a cross-sectional design, there may be potential for selection bias based on nonconsecutive sampling of patients. However, the assortment of EOS radiographs has been selected randomly which should encompass a wide spectrum of presentations. Also, this study did not take into account the reliability among individual EOS etiologies because of the relatively smaller sample size of each of these groups. Future study should address this specifically by comparing various etiologies.

## CONCLUSION

In this novel study addressing spinopelvic, thoracic and rod measurement reliability using EOS imaging, we found that most parameters have excellent inter- and intraobserver reliability. Hence, EOS imaging is an accurate and feasible tool for monitoring MCGR treatment in this population. Despite a movement towards using the ultrasound for monitoring rod distractions, radiographs are still crucial for verifying rod distracted length, measuring the degree of spinal height gain, and identifying complications. PJA assessment is shown to be unreliable for patients with an UIV cranial to T4 and thus early and accurate detection of PJK may be subject to error in this subgroup. Nevertheless, EOS imaging is still a valuable management tool with its reduced radiation exposure to a growing child.

**REFERENCES**

1. Vitale MG, Matsumoto H, Bye MR, et al. (2008) A retrospective cohort study of pulmonary function, radiographic measures, and quality of life in children with congenital scoliosis: an evaluation of patient outcomes after early spinal fusion. Spine (Phila Pa 1976) 33:1242–9.

2. Sankar WN, Acevedo DC, Skaggs DL (2010) Comparison of Complications Among Growing Spinal Implants. Spine (Phila Pa 1976) 35:2091–2096.

3. Bess S, Akbarnia BA, Thompson GH, et al. (2010) Complications of growing-rod treatment for early-onset scoliosis: analysis of one hundred and forty patients. J Bone Joint Surg Am 92:2533–43.

4. Heydar AM, Şirazi S, Bezer M (2016) Magnetic Controlled Growing Rods as a Treatment of Early Onset Scoliosis. Spine (Phila Pa 1976) 41:E1336–E1342.

5. Cheung KMC, Cheung JPY, Samartzis D, et al. (2012) Magnetically controlled growing rods for severe spinal curvature in young children: a prospective case series. Lancet 379:1967–1974.

6. Hosseini P, Pawelek J, Mundis GM, et al. (2016) Magnetically controlled Growing Rods for Early-onset Scoliosis. Spine (Phila Pa 1976) 41:1456–1462.

7. La Rosa G, Oggiano L, Ruzzini L (2017) Magnetically Controlled Growing Rods for the Management of Early-onset Scoliosis. J Pediatr Orthop 37:79–85.

8. Cheung JPY, Cahill P, Yaszay B, et al. (2015) Special Article: Update on the Magnetically Controlled Growing Rod: Tips and Pitfalls. J Orthop Surg 23:383–390.

9. Cheung JPY, Bow C, Samartzis D, et al. (2016) Frequent Small Distractions with a Magnetically Controlled Growing Rod for Early-Onset Scoliosis and Avoidance of the Law of Diminishing Returns. J Orthop Surg 24:332–337.

10. Wong CKH, Cheung JPY, Cheung PWH, et al. (2017) Traditional growing rod versus

magnetically controlled growing rod for treatment of early onset scoliosis: Cost analysis from implantation till skeletal maturity. J. Orthop. Surg. 25:

11. Cheung JP-Y, Samartzis D, Cheung KM-C (2014) A novel approach to gradual correction of severe spinal deformity in a pediatric patient using the magnetically-controlled growing rod. Spine J 14:e7-13.
12. Kwan KYH, Cheung JPY, Yiu KKL, Cheung KMC (2017) Ten year follow-up of Jarcho-Levin syndrome with thoracic insufficiency treated by VEPTR and MCGR VEPTR hybrid. Eur. Spine J.
13. Stokes OM, O'Donovan EJ, Samartzis D, et al. (2014) Reducing radiation exposure in early-onset scoliosis surgery patients: novel use of ultrasonography to measure lengthening in magnetically-controlled growing rods. Spine J 14:2397–404.
14. Cheung JPY, Bow C, Samartzis D, et al. (2016) Clinical utility of ultrasound to prospectively monitor distraction of magnetically controlled growing rods. Spine J 16:204–9.
15. Cheung JPY, Yiu KKL, Samartzis D, et al. (2017) Rod lengthening with the magnetically controlled growing rod: factors influencing rod slippage and reduced gains during distractions. Spine (Phila. Pa. 1976).
16. Abrisham SMJ, Bouzarjomehri F, Nafisi-Moghadam R, et al. (2017) A Comparison of Patients Absorption Doses with Bone Deformity Due to the EOS Imaging and Digital Radiology. Arch bone Jt Surg 5:145–148.
17. Illés T, Somoskeöy S (2012) The EOS$^{TM}$ imaging system and its uses in daily orthopaedic practice. Int Orthop 36:1325–31.
18. Pasha S, Capraro A, Cahill PJ, et al. (2016) Bi-planar spinal stereoradiography of adolescent idiopathic scoliosis: considerations in 3D alignment and functional balance. Eur Spine J 25:3234–3241.

19. Bland JM, Altman DG (1986) Statistical methods for assessing agreement between two methods of clinical measurement. Lancet (London, England) 1:307–10.

20. Michael N, Carry P, Erickson M, et al. (2017) Spine and Thoracic Height Measurements have Excellent Interrater and Intrarater Reliability in Patients with Early Onset Scoliosis. Spine (Phila. Pa. 1976).

21. Ridderbusch K, Rupprecht M, Kunkel P, et al. (2017) Preliminary Results of Magnetically Controlled Growing Rods for Early Onset Scoliosis. J Pediatr Orthop 37:e575–e580.

22. Carender CN, Morris WZ, Poe-Kochert C, et al. (2016) Low Pelvic Incidence Is Associated With Proximal Junctional Kyphosis in Patients Treated With Growing Rods. Spine (Phila Pa 1976) 41:792–797.

23. Kwan KYH, Alanay A, Yazici M, et al. (2017) Unplanned Reoperations in Magnetically Controlled Growing Rod Surgery for Early Onset Scoliosis with a Minimum of Two-Year Follow-Up. Spine (Phila. Pa. 1976).

24. Fisher A, Young WF (2008) Is the lateral cervical spine x-ray obsolete during the initial evaluation of patients with acute trauma? Surg Neurol 70:53–57.

## FIGURE LEGENDS

**Figure 1:** T1-12 length is assessed by drawing two horizontal perpendicular lines through the center of the upper endplate of the T1 vertebra and the center of the lower endplate of the T12 vertebra and then measuring the perpendicular distance between the two lines.

**Figure 2:** Measurement of pelvic inlet width is performed by a line from the widest portions of the inner pelvic ring in the posteroanterior radiograph.

**Figure 3:** Measurement of magnetically controlled growing rod (MCGR) distraction length is performed by measuring the housing unit of the MCGR actuator on the posteroanterior radiograph.

**Figure 4:** Measurement of T6 chest (a) depth on the lateral radiograph and T6 chest (b) width on the posteroanterior radiograph. The measurement is made from the inner bony border of the chest wall at the level of T6 for chest depth and from the inner bony border of the sternum to the anterior T6 vertebral body for chest width.

**Figure 5:** (a) Case example of a congenital deformity of the cervicothoracic junction. It is very difficult to properly identify the bony structures and thus (b) measurement of PJA may be subject to error.

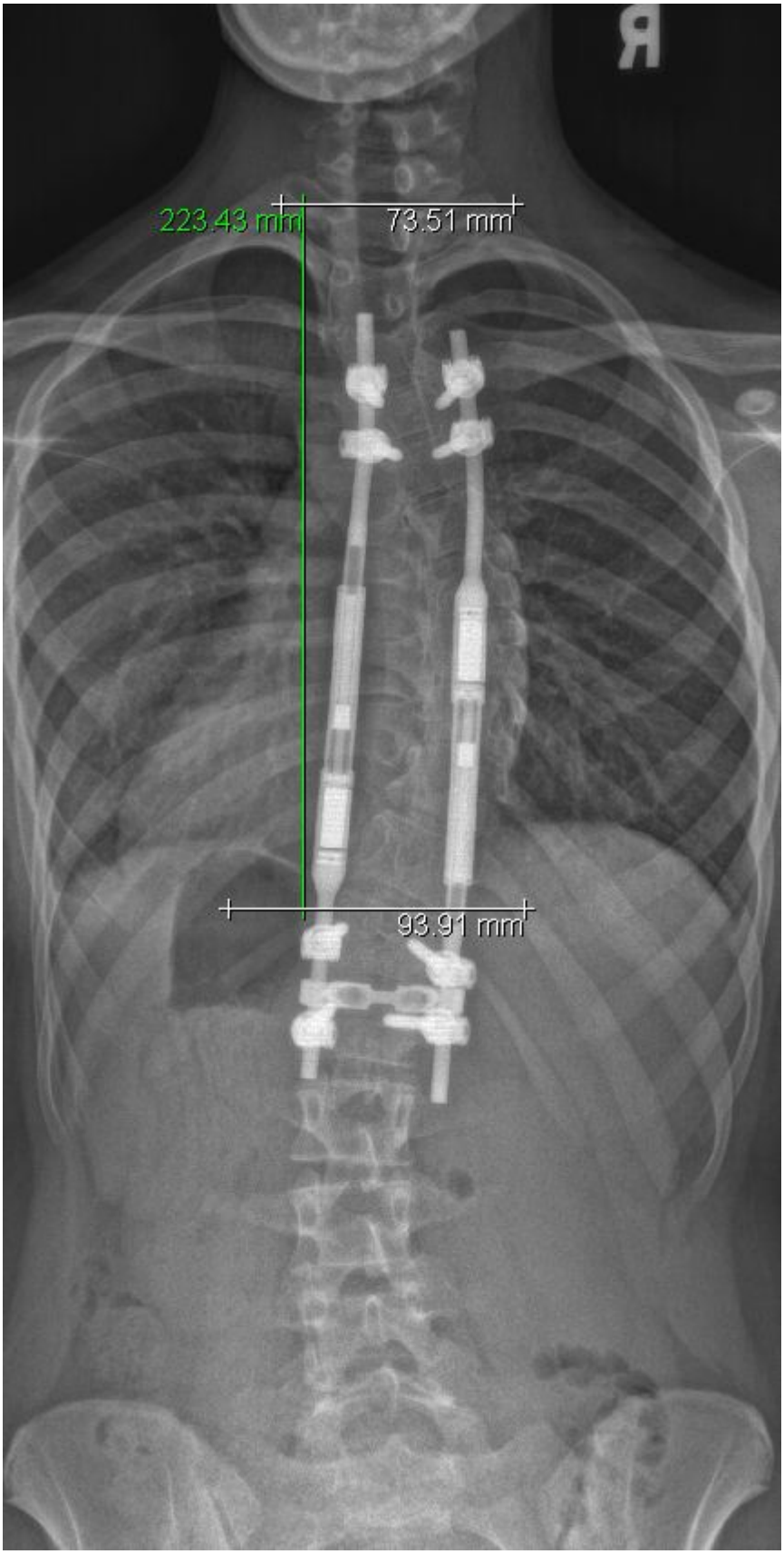


Figure 1


Figure 2

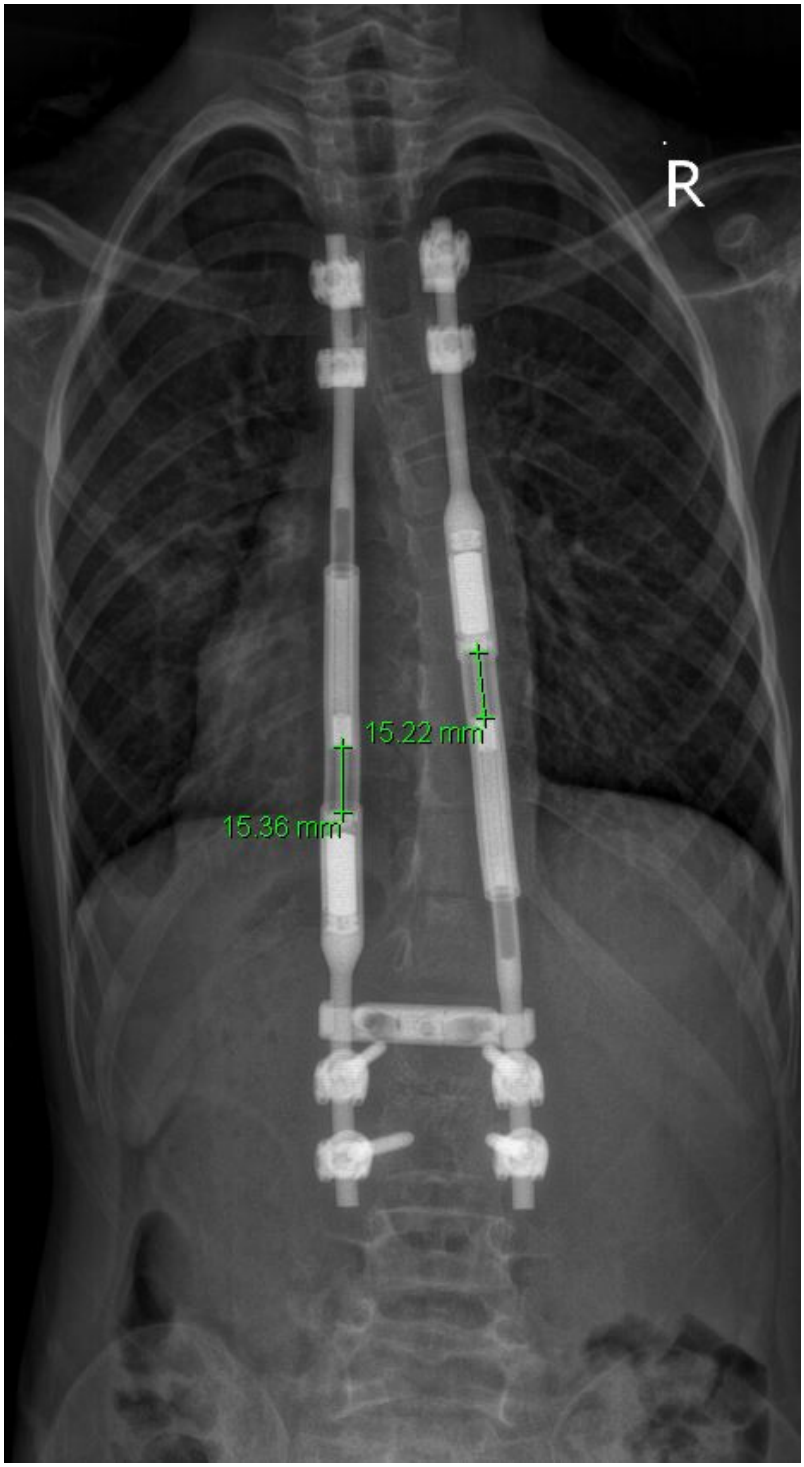


Figure 3


Figure 4b

Figure 5a,b

| Radiological Parameter | Investigator #1 Mean & SD | Investigator #2 Mean & SD | Investigator #3 Mean & SD | 95% CI | Cronbach's α | P-Value |
|---|---|---|---|---|---|---|
| Major Curve (°) | 29.18±12.49 | 29.53±10.73 | 28.46±11.29 | 0.91-0.98 | 0.96 | <0.0001 |
| Compensatory Curve (°) | 25.68±9.0 | 23.05±9.75 | 22.67±8.66 | 0.77-0.96 | 0.90 | <0.0001 |
| Coronal Balance C7-CSVL (mm) | -11.74±20.84 | -3.84±22.70 | -4.95±22.19 | 0.81-0.96 | 0.91 | <0.001 |
| Coronal T1-12 (mm) | 204.87±26.38 | 191.79±28.51 | 213.41±44.9 | 0.66-0.93 | 0.84 | <0.001 |
| Coronal T1-S1 (mm) | 346.31±39.22 | 337.55±46.56 | 336.01±46.61 | 0.82-0.96 | 0.91 | <0.001 |
| Chest width T6 (mm) | 169.90±22.50 | 170.87±20.48 | 170.01±21.13 | 0.98-0.99 | 0.99 | <0.001 |
| Pelvic inlet width (mm) | 99.56±18.24 | 101.74±17.16 | 102.14±17.23 | 0.98-0.99 | 0.99 | <0.001 |
| Left rod distracted length (mm) | 13.73±12.16 | 13.82±11.96 | 13.49±11.75 | 0.99-1.0 | 1.00 | <0.001 |
| Right rod distracted length (mm) | 12.66±11.35 | 12.90±11.32 | 12.62±11.34 | 0.99-1.0 | 1.00 | <0.001 |
| Global Kyphosis T5-12 (°) | 25.68±16.77 | 25.26±16.42 | 25.12±16.19 | 0.72-0.94 | 0.87 | <0.001 |
| Proximal Junctional Angle (°) | 3.61±3.03 | 3.92±4.32 | 3.33±2.50 | 0.71-0.81 | 0.56 | <0.016 |
| Distal Junctional Angle (°) | 17.88±11.36 | 8.53±6.13 | 14.79±9.67 | 0.774-0.95 | 0.89 | <0.0001 |
| Lordosis L1-S1 (°) | 45.07±13.32 | 44.51±11.45 | 46.19±11.44 | 0.84-0.97 | 0.93 | <0.001 |
| Sagittal Balance (mm) | 25.09±20.67 | 24.83±18.97 | 26.03±21.62 | 0.98-0.99 | 0.99 | <0.001 |
| Chest Depth T6 (mm) | 56.75±17.48 | 56.36±14.37 | 58.63±17.09 | 0.91-0.98 | 0.96 | <0.001 |
| Pelvic Incidence (°) | 41.75±10.10 | 42.54±9.93 | 43.82±10.29 | 0.95-0.99 | 0.97 | <0.001 |
| Pelvic Tilt (°) | 5.70±7.86 | 6.24±8.53 | 7.17±8.55 | 0.97-0.99 | 0.98 | <0.001 |
| Sacral Scope (°) | 36.04±8.00 | 35.45±7.63 | 35.71±7.97 | 0.98-0.99 | 0.99 | <0.001 |

Table1: Measurements for Interobserver Reliability.
Abbreviations: SD, Standard Deviation; CI, Confidence Interval

| Radiological Parameter | 1st Measurement Mean & SD | 2nd Measurement Mean & SD | 95% Ci | Cronbach's α | P-Value |
|---|---|---|---|---|---|
| Major Curve (°) | 29.18±10.73 | 29.51±11.71 | 0.82-0.97 | 0.93 | <0.0001 |
| Compensatory Curve (°) | 23.05±9.75 | 22.98±8.74 | 0.89-0.99 | 0.96 | <0.0001 |
| Coronal Balance C7-CSVL (mm) | -3.84±22.70 | -6.47±22.54 | 0.79-0.97 | 0.92 | <0.001 |
| Coronal T1-12 (mm) | 191.79±28.51 | 184.47±26.86 | 0.79-0.97 | 0.92 | <0.001 |
| Coronal T1-S1 (mm) | 337.55±46.56 | 335.96±41.03 | 0.95-0.99 | 0.98 | <0.001 |
| Chest width T6 (mm) | 170.87±20.48 | 170.73±21.22 | 0.98-0.99 | 0.99 | <0.001 |
| Pelvic inlet width (mm) | 101.74±17.16 | 102.09±17.22 | 0.99-1.00 | 1.00 | <0.001 |
| Left rod distracted length (mm) | 13.82±11.96 | 13.65±12.31 | 0.99-1.00 | 0.99 | <0.001 |
| Right rod distracted length (mm) | 12.90±11.32 | 12.65±11.52 | 0.99-1.00 | 0.99 | <0.001 |
| Global Kyphosis T5-12 (°) | 25.26±16.42 | 27.75±14.42 | 0.79-0.97 | 0.92 | <0.001 |
| Proximal Junctional Angle (°) | 3.92±4.32 | 1.76±1.22 | -1.66-0.58 | -0.53 | 0.54 |
| Distal Junctional Angle (°) | 8.53±6.13 | 9.49±5.64 | 0.60-0.94 | 0.84 | <0.0001 |
| Lordosis L1-S1 (°) | 44.51±11.45 | 45.12±12.22 | 0.80-0.97 | 0.92 | <0.001 |
| Sagittal Balance (mm) | 24.83±18.97 | 26.45±22.56 | 0.89-0.98 | 0.96 | <0.001 |
| Chest Depth T6 (mm) | 56.36±14.37 | 57.23±12.49 | 0.69-0.95 | 0.88 | <0.001 |
| Pelvic Incidence (°) | 42.54±9.93 | 43.56±9.44 | 0.90-0.99 | 0.96 | <0.001 |
| Pelvic Tilt (°) | 6.24±8.53 | 7.13±8.77 | 0.96-0.99 | 0.97 | <0.001 |
| Sacral Scope (°) | 35.45±7.63 | 36.93±7.46 | 0.84-0.98 | 0.94 | <0.001 |

Table 2: Measurements for Intraobserver Reliability.